Review

Wet and Dry Age-Related Macular Degeneration Induced by Polyethylene Glycol

Reece Mitchell , Connor Logan , Valeriy V. Lyzogubov , Nalini S. Bora , Puran S. Bora *

Posted Date: 19 July 2023

doi: 10.20944/preprints202307.1318.v1

Keywords: Age-related macular degeneration, Choroidal neovascularization, Retinal pigmented epithelium, Fluorescein isothiocyanate

Review

Wet and Dry Age-Related Macular Degeneration Induced by Polyethylene Glycol

Reece Mitchell, Connor Logan, Valeriy V. Lyzogubov, Nalini S. Bora and Puran S. Bora *

Department of Ophthalmology, Jones Eye Institute, Pat & Willard Walker Eye Research Center, 4301 West Markham, University of Arkansas for Medical Sciences, Little Rock, AR, 72205, United States; [1]rbmitchell@uams.edu, [2]cslogan@uams.edu, [3]vvlyzogubov@uams.edu, [4]nbora@uams.edu, [5]pbora@uams.edu

* Correspondence: pbora@uams.edu; Tel.: +1(501)-352-7191

Abstract: Age-related macular degeneration (AMD) is a leading cause of irreversible blindness worldwide. We recently reported that polyethylene glycol (PEG) can activate the alternative pathway of the complement system and induce choroidal neovascularization (CNV) in mice. Currently, no other investigator has demonstrated CNV after PEG injection in the mouse eye. The aim of this article is twofold: we review the histologic changes in mouse retina and retinal pigmented epithelium (RPE) after treatment with PEG, and we summarize a model of wet and dry AMD pathogenesis in mice through subretinal PEG treatment of RPE cells and retinal layers. We injected (subretinal) male C57BL/6 mice with 2 μL of solution containing 0.5 mg and 1.0 mg of PEG or PBS in control groups. Eyes were harvested at day 1, 3 and 5 after injection and processed for analysis. Sections were immunohistochemically stained for complement component C3, membrane attack complex (MAC), and cytokeratin 18. Light and laser confocal microscopy was used for image capturing. PEG increased deposition of C3 and MAC on RPE cells and on all retinal layers after 1.0 mg injection. PEG induced loss of cellular contacts between RPE cells and migration of RPE cells in the subretinal space at day 1 after PEG injection. After 0.5 mg PEG injection, increased size of RPE cells was detected at day 3 and 5. Apoptotic bodies were observed in outer nuclear layer at day 3 and 5 after 0.5 mg PEG treatment. RPE cells with dark cytoplasm and condensed chromatin were observed. Higher doses of PEG induce CNV, encouraged RPE cell proliferation and death, and damage photoreceptors in mice. This simple and fast model may be useful to explore the pathogenesis of both dry and wet AMD.

Keywords: age-related macular degeneration; choroidal neovascularization; retinal pigmented epithelium; fluorescein isothiocyanate

Introduction

Age-related macular degeneration, or AMD, is a significant and leading cause of blindness worldwide [1,2]. The early stages of AMD may exist for several years in the absence of clinically significant vision loss or ocular symptoms [2,3]. There are two key clinical subtypes of AMD: the non-exudative, or dry form, and the neovascular, or wet form. In the advanced stages of wet AMD, the development of choroidal neovascularization (CNV) leads to loss of vision and potential blindness [2,3]. CNV causes several pathologic processes, including retinal detachment, accumulation of exudates, bleeding into the subretinal space or under the retinal pigmented epithelium (RPE), and blindness resulting from photoreceptor loss [2]. As AMD progresses over time, the transition from dry AMD to primarily wet AMD is clinically significant, as pathogenic mechanisms and therapeutic strategies evolve. An improved understanding of CNV formation could aid in the creation of new therapies and treatment strategies for AMD, with particular emphasis on halting early stages of disease progression [1–3]. Currently, investigators induce CNV in animals by a variety of methods, including subretinal injection of promoting agents, laser-induces photocoagulation, debridement of

 doi:10.20944/preprints202307.1318.v1

the RPE surgically, rupture of Bruch's membrane mechanically, and transgenic or knockout animal models [4–7].

This review article aims to describe a simple and effective animal model of CNV (wet AMD) and dry AMD based on the principles of intraocular complement activation. This model can be used to understand both wet AMD pathogenesis and dry AMD development. The model induces CNV via a 1 mg subretinal injection of polyethylene glycol (PEG), an alcohol known to activate the complement system [16,17]. However, dry AMD was successfully induced by 0.5 mg subretinal injection of PEG. We are the first group to show that PEG can induce both wet AMD and dry AMD, as shown by Lyzogubov and colleagues in the Journal of Biological Chemistry in 2011 and Experimental Eye Research in 2014.

Activation of the complement activation is a significant mechanism of AMD pathogenesis in humans and animal models, and this mechanism is well-accepted in scientific literature [2,6,8–11]. Complement system activation contains a crucial event that leads to CNV: this event involves formation and accumulation of membrane attack complexes (MAC) on choroidal and RPE cells [8–10,12,13]. MAC deposition in turn induces production and secretion of vascular endothelial growth factor (VEGF), a key angiogenic mediator of CNV proliferation [8,12]. Additionally, MAC has been associated with causing cell death [13,14]; however, sub-lytic MAC concentrations have been shown to stimulate cellular production, generate inflammation, and alter cellular functioning [14,15].

Phospholipid-methoxyPEG conjugate activates the complement system through the classic and alternative pathway [17]. PEG is used ubiquitously in small quantities in cosmetics and pharmaceutical delivery systems [18–20]. Within pharmacologic applications, low weight PEGs are absorbed rapidly and excreted through the urine. PEG is eliminated from the body almost entirely within the first 24 hours after administration, and PEG undergoes little to no significant metabolism in vivo [20]. So far, no reports describe PEG as an inducer of dry AMD or an activator of the complement system in the eye to induce neovascularization or angiogenesis. We described PEG's role in dry AMD pathogenesis and the angiogenic effects administering PEG via subretinal injection. Additionally, we explored the early stages of CNV as influenced through complement activation by PEG.

Dry AMD is often described as an "early stage" within the progression of AMD. Features of dry AMD are characterized by lipofuscin accumulation in the RPE, decreased numbers of RPE cells, and thickening of Bruch's membrane with loss of associated structure [21]. The hallmark sign of dry AMD is the formation of subretinal lipid and protein depositions known as drusen. Studies have identified various components of drusen, including lipids, complement factors (C3, C5, C5b-9, CFH), and acute-phase reactants [2,22,23]. Within the "advanced stage" of AMD, characteristic findings of RPE cell hypertrophy and calcification of Bruch's membrane may be visualized. This calcification plays a key role in the development of choroidal neovascularization. In CNV, new vessels are formed under the RPE and is the hallmark sign of wet AMD. While the treatment of wet AMD is well-researched, there is a paucity of literature examining the treatment of dry AMD. Clinically relevant animal models are highly desirable for understanding the mechanisms underpinning the early stages of dry AMD, which may lead to new therapeutic strategies.

Subretinal injection of PEG

We have shown that PEG can induce CNV in mice [24], and we described the effects of 0.5 mg PEG, when injected subretinally, on retinal thickness, RPE cells, the retina, and regulation of expression of some genes [25,26]. For subretinal injection, a 27G needle was used to decompress the mouse eye via insertion through the conjunctiva and sclera 1mm behind the limbus. For injections, a UMP3 Microinjector equipped with a Nanofil 100 μL syringe and 33G blunt needle was used as previously described [10]. Upon encountering light resistance, needle movement was stopped.

To investigate dose-dependent effects of PEG, we divided mice into 7 groups, with 3 mice per group. As controls, one group was not treated, and Group 2 received a single subretinal injection of sterile PBS. Five experimental groups were injected with varying PEG doses: 2.0 mg, 1.0 mg, 0.5 mg, 0.25 mg, and 0.125 mg. PEG doses were dissolved into sterile PBS before injection, and the volume of

 doi:10.20944/preprints202307.1318.v1

all injections was 2 μL. In each experiment, a single injection was applied. Minor retinal detachment occurred in some subretinal injections. After optimizing the PEG dose needed for CNV stimulation, mice received a 1.0 mg subretinal PEG injection. Mice from each of the 7 groups were sacrificed on days 1, 3, 4, 5, 7, 14, 21, 28 and 42 after injection. CNV size was measured as previously described [8–10,26]. Sacrificed animals were perfused with 0.75 ml of PBS containing 50 mg/ml of fluorescence-labeled dextran. To reconstruct three-dimensional CNV sites, 1 μm thick flat mounts were captured and compiled into Z-stack images, and a projection tool was applied to create an X view of corresponding Z-stack images. CNV within subretinal tissue was identified between two RPE layers stained positive for cytokeratin 18.

Histological Studies

Histological analyses of harvested mouse eyes were completed as described by Lyzogubov et al [10]. After completing subretinal PEG and PBS injections, five mice per time point were sacrificed on days 1, 3, and 5 post-injection. All harvested eyes were fixed with buffered, pH neutral formalin. Two eyes from each group were embedded in a block of composite paraffin, from which serial 5-μm sections were cut. Sections were H&E stained and subsequently used for immunohistochemistry staining. An additional collection of four eyes from each group were treated with 2.5% glutaraldehyde in 0.05 M cacodylate buffer Eyes were then post-treated in 1% osmium tetroxide and implanted in epon 812 resin. Sections were cut in widths of 1 μm and stained with Epoxy Tissue Stain. Immunohistochemical antibodies were utilized, including goat polyclonal anti-complement 3 antibody, rabbit-derived polyclonal anti-MAC (C9 neoepitope) antibody, and goat polyclonal antibody against VEGF165 antibody. Mouse monoclonal anti-cytokeratin 18 IgG1 and phallotoxin-Alexa Flour (AF)594 was used for RPE cell identification. Four eyes from each group were prepared as described above, but 1 μm sections were cut and stained using hematoxylin.

Microscopy and image analysis

Slides of paraffin sections stained with H&E were examined using an Olympus microscope equipped with a QImaging GO-5 camera. Three images from each eye section were captured with a 40x objective. Image resolution was 2592 x 1944 pixels (px) and the size of captured images was 235 x 175 μm (11 px/μm). Image analysis was performed with the ImageJ program. The total number of nuclei in the outer nuclear layer (ONL) was counted, and the retinal length at the level of outer limiting membrane was measured. From these data, the number of ONL nuclei per 1 mm of retinal length was determined. Similarly, the number of nuclei in the RPE layer was counted, and the length of the RPE layer at the level of the cells' basal surface cells was measured. The number of RPE cell nuclei per 1 mm of RPE layer length was calculated. We measured the height of RPE cells from basal to apical surface as well as the length of photoreceptors from outer limiting membrane to their outermost part facing either choroid or RPE cells. Data were analyzed and compared with Student's t-test test; differences were considered statistically significant with $p<0.05$.

CNV induction after PEG injection

CNV of different sizes was observed in all PEG-injected groups. However, CNV was rare and limited to single vessel neovascularization over very small areas in the group injected with 0.125 mg PEG. Relative to this group, CNV was larger in the group injected with 0.25 mg, and CNV was even larger in the group injected with 0.5 mg (data not shown). The higher dose of 1.0 mg (Figure 1b,c) stimulated advanced CNV across a greater area. A dose-dependent relationship between increased PEG and CNV was observed. No CNV was observed in control animals injected with equivalent volumes of sterile PBS (Figure 1a).

Preprints (www.preprints.org) | NOT PEER-REVIEWED | Posted: 19 July 2023 doi:10.20944/preprints202307.1318.v1

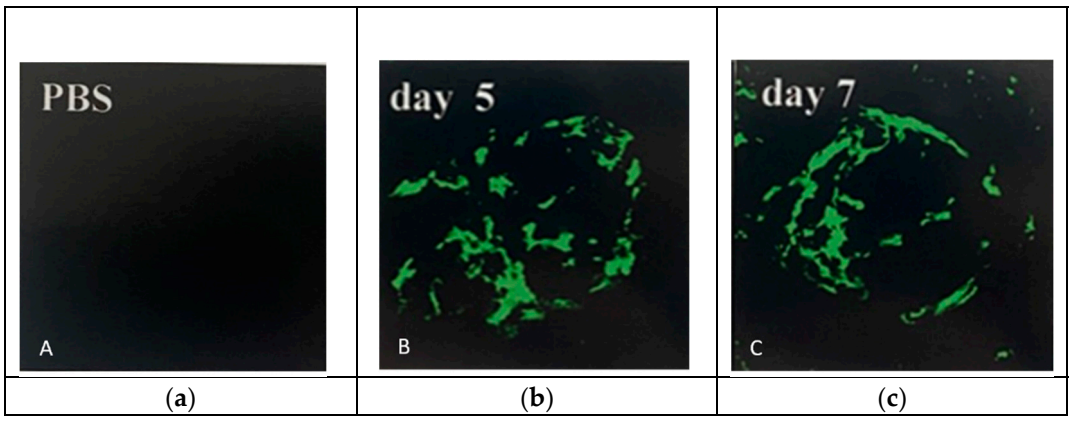

Figure 1. C57BL/6 mice were sacrificed on day 5 and 7 after 1.0 mg subretinal PEG or PBS injection. (a) No CNV was detected in the PBS injected animals at any time point; (b) CNV was detected 3 days after treatment with PEG, increased in size until day 5 after injection, and persisted up to 42 days; (c) CNV was consistent in size between days 5 and 14, but started decreasing from day 21 until day 42. Figures were previously published by Lyzogubov et al. in the Journal of Biological Chemistry in 2011 [24].

When examining mice treated with PBS, vessels supplied with FITC-dextran were present within the choroid and under RPE cells stained positive for cytokeratin 18 (Figure 2a). CNV in PEG-injected animals was localized between two layers of RPE cells (Figure 2b).

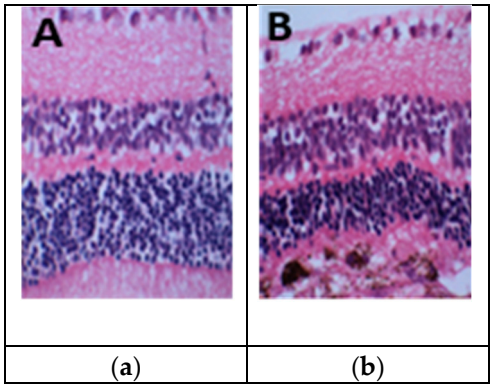

Figure 2. Treatment of PBS (a) showed no change in outer nuclear layer (ONL) and photoreceptor (POS) outer and inner segments; (b) PEG 0.5mg changed the size of RPE, reduced the size of photoreceptor (POS) outer and inner segments, ONL and outer limiting membrane (OML). Figures were previously published by Lyzogubov and colleagues in Experimental Eye Research in 2014 [25].

Investigation of 1 μm epon-embedded sections from PBS-treated mice showed containment of choroidal vessels within the choroid and an RPE consisting of a single cell layer. In comparison to control mice, mice injected with PEG had increased average RPE cell size and spacing between adjacent cells. CNV was localized on day 5 after PEG injection between two RPE cell layers within the subretinal space. Importantly, no vessels of retinal origin were present in this layer. Paraffin sections were taken from mice injected with PBS and PEG 1, 3, and 5 days after treatment and immunohistochemically stained for endothelial cell marker Isolectin-IB4. PBS-treated groups contained a single layer of RPE cells and appropriately localized choroidal endothelial cells. Isolectin-IB4–positive endothelial cells were found between RPE cells after 1 day of PEG treatment. Isolectin-IB4-positive endothelial cells demonstrated invasion of preexisting choroidal vasculature, Bruch's membrane, and intercellular RPE space. Three days after the injection, neovascular formations from subretinal endothelial cells had formed, and additional RPE cells had formed into a second layer. The newly developed vessels formed a CNV complex 5 days after the PEG injection within the subretinal space (Figure 3a–d) [25].

Preprints (www.preprints.org) | NOT PEER-REVIEWED | Posted: 19 July 2023 doi:10.20944/preprints202307.1318.v1

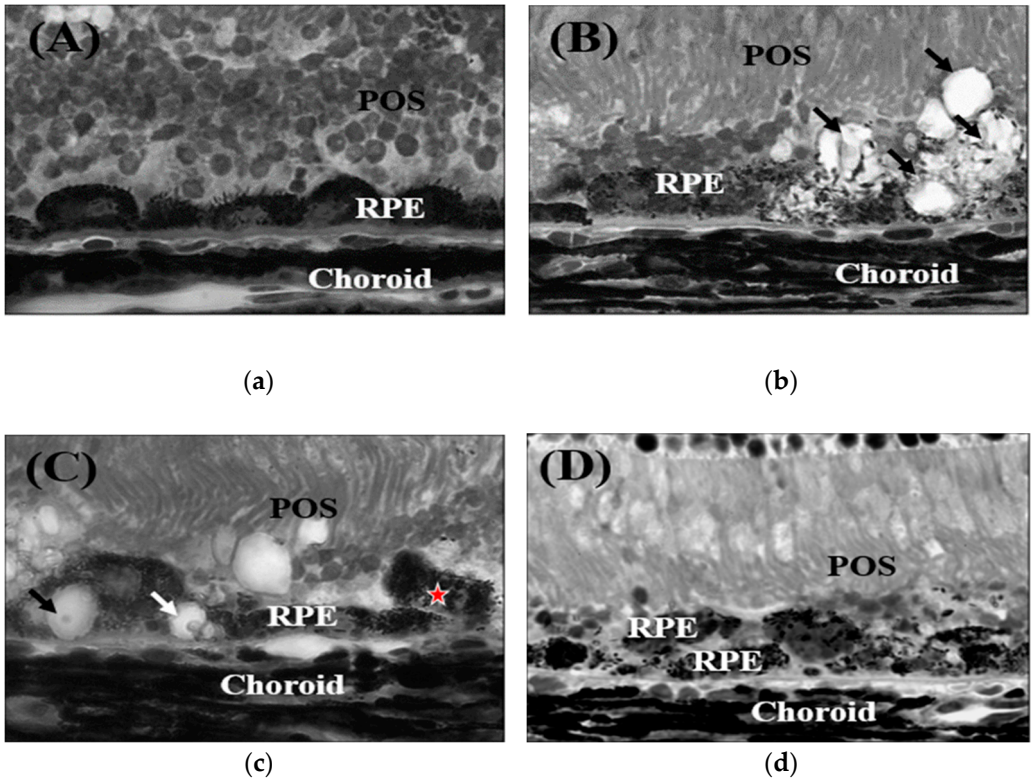

Figure 3. Sub-retinal injection of PEG. Day 1 after injection. Epon (1 um) section of mouse RPE-choroid stained with hematoxylin. (a) RPE cells become round and oval shape; (b) some RPE cells form vacuoles (white arrow); (c) vacuoles in RPE cells contain debris (black arrow), while some RPE cells migrate between RPE and POS (star); (d) two layers of RPE cells are formed [25].

Retinal changes after 1-mg PEG injection

On day 5 after injection with PBS or PEG, paraffin sections were histologically investigated for retinal variations. We found that PEG decreased the number of photoreceptor cell nuclei located in ONL, shortened the size of photoreceptor outer and inner segments, increased the number and size of RPE cells, and reduced pigmentation of RPE cells (Figure 3a–d) [24].

In the first part of the experiment, dose-dependent effects of PEG on retinal ONL thickness were explored by subretinal injection with PBS or with 0.025, 0.25, 0.5, or 1.0 mg of PEG. Mice were sacrificed 5 days after injection with PEG, using 5 mice per group. Paraffin sections of 5 μm thickness were harvested from mouse eyes and stained with H&E. Measurement of ONL thickness revealed that both 0.5 and 1.0 mg doses of PEG significantly reduced thickness of the ONL based on ANOVA testing, with $p<0.05$. For the second portion of the experiment, time-dependent effects of PEG on retinal ONL thickness were examined using the minimal effective dose of subretinal 0.5 mg PEG or PBS injection. Five mice from each group of animals injected with PEG or PBS were sacrificed after injection on days 1, 3, 5, and 14. Measurement of ONL thickness demonstrated that PEG-injected animals had significantly thinner ONL on days 5 and 14 than did PBS-treated controls according to ANOVA testing with $p<0.05$. From these results, 0.5 mg PEG injections were utilized for further experimentation, and animals were sacrificed 5 days after receiving injection.

Apoptosis of photoreceptors has been described in most degenerative diseases of the retina, including dry AMD [15,27]. We hypothesized that subretinal PEG injection decreased ONL thickness via apoptotic photoreceptor death. In order to investigate this hypothesis, we used paraffin sections to perform TUNEL assays and immunohistochemistry studies of caspase 3 active (Casp3act). We also performed histological investigations of plastic sections by light and electron microscopy. TUNEL-positive nuclei were identified within the retinal ONL in eyes injected with both PBS and PEG. After quantifying TUNEL-positive nuclei with ANOVA testing with $p<0.05$, results demonstrated a

 doi:10.20944/preprints202307.1318.v1

significant increase in the apoptotic index of PEG treated eyes in comparison to PBS treated controls on days 3 (5.4+1.19%) and 5 (6.8+1.99%) after injection. The apoptotic index was determined from the percent of TUNEL-positive nuclei. Co-localization studies comparing TUNEL staining and Casp3act staining occurred in eyes on day 5 after PEG injection. TUNEL positive nuclei strongly co-localized with cytoplasmic and nuclear staining for Casp3act.

We observed chromatin condensation, nuclear fragmentation, and formation of apoptotic bodies in the ONL of PEG treated eyes by light and electron microscopy. Eyes treated with PBS lacked these apoptotic signs (not shown). Our results also showed a striated pattern in photoreceptor outer segments (POS) in PBS-treated eyes due to the presence of numerous lamellae. Microscopic investigation of PEG-injected eyes revealed reduced POS length. Photoreceptor inner and outer segment lengths (PIS/POS) of PEG- and PBS-treated animals was measured on paraffin sections stained with H&E, revealing a significant 61% decrease in PIS/POS length in eyes injected with PEG compared to PBS (t-test, $p<0.05$). Additionally, a significant decrease in ONL nuclear density of 49% was noted in eyes injected with PEG compared to PBS on H&E-stained paraffin sections (t-test, $p<0.05$).

Mouse models provide a useful methodological framework for exploring mechanisms and pathways of various pathologies [28]. This is in large part due to the development of transgenic and knockout strains, which can be used to model specific disease processes. Several models have been developed to model retinal pathologies, including CNV [29–31]. Experimental findings from these models have aided efforts in developing potential therapeutic and causative agents of retinal disease and CNV. One such compound is PEG, which has been demonstrated to activate the complement system and lead to morphological changes consistent with dry AMD in the retina. Furthermore, PEG can induce RPE proliferation as well as RPE and photoreceptor death in mice. This agent is a simple and fast model for investigating dry AMD pathogenesis.

The hallmark sign of wet-type AMD is choroidal neovascularization. The macula plays a key role in human central vision. The macula is highly dependent on the choroidal blood supply, and this dependency represents an "Achilles' heel" of the human eye. With natural aging and a combination of various risk factors, the unique organization of macular vascularization becomes adversely affected. Uncontrolled growth of choroidal vessels can lead to and often irreversible changes in interactions of photoreceptors, RPE, and choroid [1,3]. Untreated wet AMD can rapidly progress from decreased visual acuity to central blindness and dramatically impact quality of life. A robust understanding of CNV formation at a mechanistic level will further efforts to develop improved treatment modalities for AMD.

We present an effective, affordable, and simple model of CNV in mice utilizing a single injection of subretinal PEG. After injection, PEG spreads between the RPE and neuronal retinal layers. This is confirmed under microscopy by visualization of a subretinal bleb. The resulting changes in retinal structure in this accelerated model resemble features of wet AMD. The initial stages of CNV were identified as arising from preexisting choroidal capillaries 1 day after PEG injection. These initial phases include the following findings: formation of vascular sprouts from pre-existing choroidal capillaries, RPE cell enlargement and disruption of intercellular contacts, and penetration into Bruch's membrane in several sites [1]. Formation of new vessels was noted in the subretinal space on day 3 after treatment. On day 5, complexes of CNV reached their maximally observed size and began decreasing after day 14. Currently, there has been limited investigation into the initial stages of CNV [1]. An important component of early CNV is described as subclinical CNV, where endothelial cells and fibrovascular tissues proliferate extensively into the subretinal space or under the RPE via gaps in the Bruch's membrane. [1,32]. This pathology is presents with absent characteristic signs on funduscopic examination. Additional signs of early AMD include the formation of drusen as well as hyperpigmentation and degeneration of the RPE [3].

Identifying early signs of CNV poses considerable difficulty, given a lack of observable funduscopic changes prior to the onset of early AMD. Animal models are necessary to investigate the early microscopic events contributing to CNV development and progression. Previously, injections of various agents in the subretinal space have been used to induce CNV. A wide variety of

 doi:10.20944/preprints202307.1318.v1

compounds have been investigated in several animal models, including lipid hydroperoxide within rats injection of rabbits with autologous vitreous and microspheres containing basic fibroblast growth factor, or microspheres containing VEGF within monkeys [4–7,33]. Induction of CNV by laser photocoagulation is frequently utilized in several species models [4–6,8–10], which achieves CNV induction due to laser-induced damage to RPE cells, Bruch's membrane, and choroid. In comparison to laser-induced models of CNV, subretinal PEG injection produces less damage to the RPE and choroid. A similar model of CNV that uses subretinal injection of matrigel has been described for use in rats [34,35].

PEG has demonstrated significant complement system activation and especially of the alternative pathway [16]. Dose-dependent effects of PEG on increased CNV size have been observed, and we propose that increased PEG doses lead to greater complement component C3 hydration and subsequent alternative pathway activation. We identified local activation of the complement system after subretinal PEG injection without systemic bloodstream complement activation via staining RPE-choroid for MAC (C9 neoepitope) [24].

These findings support the hypothesis that CNV induction requires complement system activation in the PEG-induced model [2,8–11]. Deposition of the complement component C3 and increased levels of C3 split products were detected at high levels 1 day after PEG treatment in within choroidal and RPE tissues, thereby confirming complement system activation. Major split products of C3 with molecular weights of 23 kDa and 43 kDa are potential components of the iC3b α chain or C3c protein, and the presence of these complement split products indicate an inflammatory state in the choroid [36]. Over time, reduction in the 23 kDa split product on days 3 and 5 after PEG injection indicate increased destruction of this split product [24]. Complement system activation stimulated deposition of MAC, with resulting increases in expression and secretion of growth factors. RPE and endothelial cells responded to these growth factors via migration, proliferation, and cellular transformation.

We discovered that CNV is initiated by an acute and high degree of local complement activation due to PEG injection in the posterior pole of the mouse eye. Previous literature has demonstrated that factor B, H and C2 mutations increase risk of CNV and AMD, as well as drusen formation and dry AMD [37–39]. Additional literature published by Rohrer and coworkers has confirmed an association between increased RPE oxidative injury and VEGF production due to chronic, sub-lytic complement system activation [23].

There are several advantages of this proposed model of CNV induction via subretinal PEG injection: 1) mice are economical and easy to handle; 2) CNV induction with PEG is inexpensive and easy to perform; 3) PEG-induced CNV occurs quickly within 3 days and for a limited time period; 4) subretinal PEG injection is less traumatic to retinal architecture than laser or surgical disruption; 5) pathological changes are limited to the posterior pole; and 6) PEG injection stimulates VEGF expression and mimics the pathologic changes of human AMD. Of note, the CNV produced from PEG injection in mice mirrored human AMD remarkably well, regardless of cellular composition, morphology, and other etiologic factors [7]. While significant differences exist between this mice model and human AMD in terms of an accelerated time course for modeling CNV, absence of a macula in mice, and the significant effects of human risk factors for AMD pathogenesis, the proposed model of CNV remains useful for investigating mechanisms of CNV formation. Moreover, this model is well adapted to examine the effect of potential inhibitors of neovascularization in AMD. Previously, PEG was described as having an angiogenic effect in relation to myocardial ischemia [40] and other similar results [41]. However, there has been no previous investigation into PEG and inducing CNV prior to this study. This study provides a new avenue for applying PEG-induced angiogenesis to model AMD. Furthermore, this study affirms the angiogenic properties of PEG and has broader implications for exploring the process of wound healing, which often necessitates rapid revascularization and angiogenesis.

Preprints (www.preprints.org) | NOT PEER-REVIEWED | Posted: 19 July 2023 doi:10.20944/preprints202307.1318.v1

Dry AMD like changes after 0.5-mg PEG injection

Dry AMD displays hallmark signs of retinal RPE degeneration. Our results clearly demonstrated that when compared to PBS controls, RPE cell nuclei density was significantly increased in mouse eyes treated with PEG. The results of our investigation show similarity between the pathological changes seen in PEG injected mouse eyes and those seen in dry AMD with humans. A subretinal injection of 0.5 mg PEG enabled the development of several signs of dry AMD at a time point of 5 days after treatment. The RPE and retinal neuron layers were closely investigated. PEG demonstrated significant effects on ONL photoreceptors. As a result of caspase-dependent apoptosis of photoreceptors, ONL cell density, thickness, and PIS/POS lengths decreased. Importantly, human dry AMD exhibits similar retinal photoreceptor losses during its pathogenesis. Retinal and RPE pathological changes occurred in parallel within the PEG injection model. After injection of PEG, we found degeneration in the form of depigmentation, size reduction, accumulations of membrane components within phagosomes, and structures resembling drusen. Additionally, proliferation of RPE cells was also noticed after PEG injection, which may be attributed to complement system activation [11]. Accumulation of C3 and MAC, as well as the actions of other complement system components may lead to RPE cell dysfunction [24,25].

RPE degeneration and activation of autophagy by PEG

Mouse eyes were stained with basic fuchsin and toluidine blue and examined in 1 μm plastic sections using light microscopy. From microscopic examination, PBS-injected control mice contained a single uniform layer of RPE cells with attachment to Bruch's membrane and a parallel nuclear orientation [25]. In mouse eyes injected with PEG, the RPE experienced significant changes including degeneration, depigmentation, reduced thickness, and deposition of structures resembling drusen. Atg12 was applied to 5 μm paraffin sections of eyes injected with PEG and PBS in order to highlight regions of autophagy. PEG injected eyes showed increased regions of Atg12 expression and autophagy in comparison to PBS control. PEG-treated eyes were examined with electron microscopy, showing macroautophagosomes containing vesicles, pigmented granules, and mitochondria located in the cytoplasm between the nuclear or cytoplasmic and cellular membranes of RPE. Vesicles in autophagosomes exhibited a double-layered pattern [25]. RPE depigmentation was associated with two crucial processes: RPE proliferation and autophagy. During autophagy, digestion of cytoplasmic components and pigmented granules contributes to RPE depigmentation. Increased RPE cellular proliferation and dedifferentiation may also lead to decreased pigmentation. RPE depigmentation decreases their protective function and reduces retinal support and nutrition. Photoreceptor depth and resulting debris is another factor that affects RPE, where phagosomes containing POS and photoreceptor fragments overload the RPE. Increased phagocytosis and autophagy may lead to lipofuscin accumulation—an important player in dry AMD pathogenesis. We found a link between drusen-like structures seen with light and electron microscopy (Figure 4a,b).

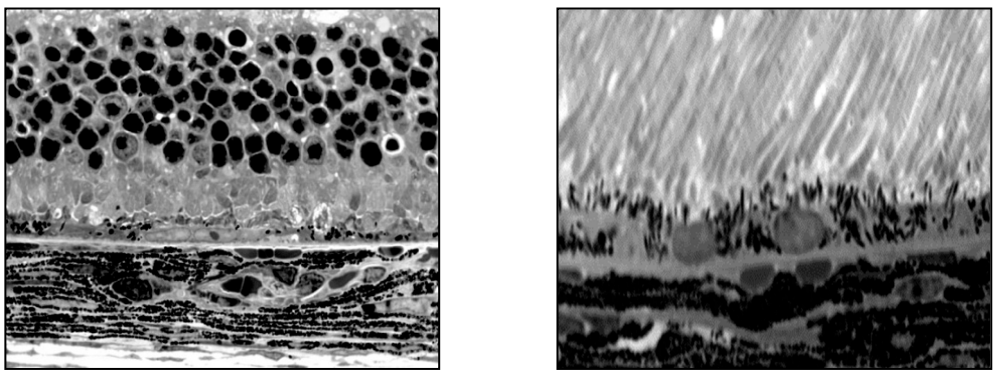

(**a**) (**b**)

Figure 4. (a) Normal retina, intact RPE, photoreceptors, and outer nuclear layer; (b) Damaged retina, few RPE, and damaged choroid and photoreceptors due to treatment with 0.5 mg of PEG [25].

 doi:10.20944/preprints202307.1318.v1

After subretinal injection of 0.5mg PEG, the RPE, choroid, and retinal photoreceptors experienced significant damage and loss of normal architecture, consistent with dry AMD findings. Specific findings include loss of regular structure of tissue layers, as well as formation of macroautophagosomes within the RPE. Vacuolization was also noted within the RPE and choroidal layers, and these cytologic findings provide evidence of RPE, choroidal, and retinal photoreceptor degeneration [25]. The progression of macroautophagosome and vacuole formation after 0.5mg PEG injection provides evidence that the degenerative changes seen in dry AMD may be replicated by subretinal PEG injection.

Reliability and reproducibility of PEG injection as a basis for AMD

Other research groups have examined the reliability of inducing CNV via subretinal PEG injection. In a study aimed at examining the reliability and reproducibility of inducing CNV according to Lyzogubov et al., Fernando-Bueno and colleagues found inconsistency in the ocular changes described in PEG and PBS-injected mice [42]. Specifically, they identified early histological signs of CNV within PEG-injected mice, including degenerative changes in the external retinal layer, disruption of the RPE and choroid with vacuolization, and increased IB4 immunoreactivity. These findings were consistent with reported findings from Lyzogubov et al. However, these findings were heterogeneous and inconsistent within PEG-injected mice, and some of the early signs of CNV were also present in PBS-injected mice [42]. Moreover, no significant VEGF or von Willebrand factor (vWF) activity was identified in PEG or PBS injected mice on day 14 after injection [42]. This report differs significantly from previously described dose-dependent effects of PEG on CNV and the important absence of CNV within PBS-injected mice (Figure 1). The reported presence of retinal changes consistent with early CNV in PBS and PEG-injected mice may indicate retinal trauma secondary to subretinal injection as a potential confounding source of CNV induction [43].

Conclusions

From the reviewed literature related to PEG-induced CNV and dry AMD in mice, this model provides a potential route for investigating the both the pathogenesis CNV and of drusen formation. RPE cells form the main retinal blood barrier, and it is critically important for this barrier to maintain a functional state. Transformation and proliferation of RPE may be a compensatory mechanism to replace degenerative non-functional RPE. On the other hand, proliferation of RPE may lead to disruption of the retinal blood barrier. Some of the genes upregulated in PEG-injected animals were similar to those upregulated in human AMD, supporting the potential utility of this model for studying dry-type AMD [25].

We conclude that morphological changes caused by 0.5 mg PEG in RPE and the retina are consistent with human dry AMD. PEG is a useful tool for inducing proliferation and death of RPE cells. This simple, quick model may be useful for investigating the pathogenesis of dry AMD. The methods described above for subretinal injection of 1.0 mg PEG will generate a CNV model consistent with wet AMD, and the subretinal injecting of 0.5 mg PEG will generate a model of dry AMD. This model is cost-effective, less invasive, and less painful than laser induced CNV models. Additionally, subretinal PEG injection carries the added benefit of having the ability to generate predominantly wet or dry AMD findings, simply by altering the PEG dose. Future efforts aimed at producing mixed features of wet and dry AMD through subretinal PEG injection may improve our understanding of how mechanisms of dry and wet AMD potentially influence one another. Findings from PBS and PEG-injected mice warrants additional investigation into potential confounding factors related to CNV induction from subretinal injection, including localized trauma and inflammation of retinal and choroidal tissues. Given the ease, cost effectiveness, and minimally invasive nature of subretinal PEG injection as a platform for inducing wet or dry AMD, this mouse model warrants continued research and eventual implementation as an option for exploring AMD pathogenesis. The ability to quickly generate features of dry or wet AMD through subretinal PEG injection in mice could advance the mechanistic understanding of AMD and the development of pharmaceutical therapies.

Author Contributions: Puran Bora conceived of the idea. Puran Bora, Reece Mitchell, Connor Logan, Valeriy Lyzogubov, and Nalini Bora wrote in parts and edited the manuscript.

Acknowledgement: This article was edited by Margaret (Peggy) Brenner for English language. Peggy is our (University of Arkansas for Medical Sciences) English language and scientific editor.

Institutional Review Board Statement: Not applicable.

Data Availability Statement: Not applicable.

Funding: This work was funded by grants from the University of Arkansas for Medical Sciences and the Pat and Willard Walker Eye Research Center, Little Rock, AR, 72205.

Conflicts of Interest: The authors have no conflicting interests to disclose.

Abbreviations Used: CNV, choroidal neovascularization; AMD, age-related macular degeneration; RPE, retinal pigmented epithelium; ONL, outer nuclear layer; H&E, hematoxylin and eosin; FITC, fluorescein isothiocyanate; PEG, polyethylene glycol; MAC, membrane attack complex; VEGF, vascular endothelial growth factor; PIS, photoreceptor inner segments; POS, photoreceptor outer segments.

References

1. Campochiaro, P. A. Retinal and Choroidal Neovascularizatoin. *J. Cell. Physiol.* **2000**, 184, 301–310
2. Coleman, H. R.; Chan, C. C.; Ferris 3rd, F. L.; and Chew, E. Y. Age-related macular degeneration. *Lancet.* **2008**, 372(9652), 1835–1845
3. Zarbin, M. A. Current concepts in the pathogenesis of age-related macular degeneration. *Arch. Ophthalmol.* **2004**, 122(4), 598–614
4. Montezuma, S. R.; Vavvas, D.; and Miller, J. W. Review of ocular angiogenesis animal models. *Semin. Ophthalmol.* **2009**, 24(2), 52–61
5. Elizabeth Rakoczy, P.; Yu, M. J.; Nusinowitz, S.; Chang, B.; and Heckenlively, J.R. Mouse models of age-related macular degeneration. *Exp. Eye Res.* **2006**, 82(5), 741–752
6. Edwards, A. O.; and Malek, G. Molecular genetics of AMD and current animal models. *Angiogenesis.* **2007**, 10(2), 119–132
7. Lassota, N. Clinical and histological aspects of CNV formation: studies in an animal model. *Acta Ophthalmol.* **2008**, 86, 1–24
8. Bora, P. S.; Sohn, J. H.; Cruz, J. M.; Jha, P.; Nishihori, H.; Wang, Y.; Kaliappan, S.; Kaplan, H. J.; and Bora, N. S. Role of complement membrane attack complex in laser-induced choroidal neovascularization. *J. Immunol.* **2005**, 174(1), 491–497
9. Bora, N. S.; Kaliappan, S.; Jha, P.; Xu, Q.; Sohn, J. H.; Dhaulakhandi, D. B.; Kaplan, H. J.; and Bora, P. S. Complement activation via alternative pathway is critical in the development of laser-induced choroidal neovascularization: role of factor B and factor H. *J. Immunol.* **2006**, 177(3), 1872–1878
10. Lyzogubov, V. V.; Tytarenko, R. G.; Jha, P.; Liu, J.; Bora, N. S.; and Bora, P. S. Role of ocular complements factor H in a murine model of choroidal neovascularization. *Am. J. Pathol.* **2010**, 177(4), 119–129
11. Anderson, D. H.; Radeke, M. J.; Gallo, N. B.; Chapin, E. A.; Johnson, P. T.; Curletti, C. R.; Hancox, L. S.; Hu, J.; Ebright, J. N.; Malek, G.; Hauser, M. A.; Rickman, C. B.; Bok, D.; Hageman, G. S.; and Johnson, L. V. The pivotal role of the complement system in aging and age-related macular degeneration: hypothesis re-visited. *Prog. Retin. Eye Res.* **2010**, 29(2), 95–112
12. Seddon, J. M.; Yu, Y.; Miller, E. C. et al. Rare variants in CFI and C9 are associated with high risk of advanced age-related macular degeneration. *Nat. Genet.* **2013**, 45, 1366–1370
13. Ramo, K.; Cashman, S. M.; and Kumar-Singh, R. Evaluation of adenovirus-delivered human CD59 as a potential therapy for AMD in a model of human membrane attack complex formation on murine RPE. *Invest. Ophthalmol. Vis. Sci.* **2008**, 49(9), 4126–4136
14. Morgan, B. P. Complement membrane attack on nucleated cells: resistance, recovery and non-lethal effects. *Biochem. J.* **1989**, 264(1), 1–14
15. Halperin, J. A.; Taratuska, A.; and Nicholson-Weller, A. Terminal complement complex C5b-9 stimulated mitogenesis in 3T3 cells. *J. Clin. Invest.* **1993**, 91(5), 1974–1978
16. Hamad, I.; Hunter, A. C.; Szebeni, J.; and Moghimi, S. M. Polyethylene glycols generate complement activation produces in human serum through increased alternative pathway turnover and a MASP-2-dependent process. *Mol. Immunol.* **2008**, 46(2), 225–232
17. Moein, M. S.; Hamad, I.; Bünger, R.; Andresen, T. L.; Jørgensen, K.; Hunter, A.C.; Baranji, L.; Rosivall, L.; and Szebeni, J. Methylation of the phosphate oxygen moiety of phospholipid-methoxy (polyethylene glycol) conjugate prevents PEGylated liposome-mediated complement activation and anaphylatoxin production. *J. Liposome Res.* **2006**, 16(3), 167–174

18. Veronese, F. M.; and Pasut, G. PEGylation, successful approach to drug delivery. *Drug Discovery Today.* **2005**, 10(21), 1451–1458
19. Yamaoka, T.; Tabata, Y.; and Ikada, Y. Fate of water-soluble polymers administered via different routes. *J. Pharm. Sci.* **1995**, 84(3), 349–354
20. Final report on the safety assessment of Triethylene Glycol and PEG-4. *Int. J. Toxicol.* **2006**, 25, 121–138
21. Sarks SH. Aging and degeneration in the macular region: a clinico-pathological study. *Br. J. Ophthalmol.* **1976**, 60(5), 324–341
22. Nozaki, M.; Raisier, B.J.; Sakurai, E.; Sarma, J.V.; Barnum, S.R.; Lambris, J.D.; Chen, Y.; Zhang, K.; Ambati, B.K.; Baffi, J.Z.; Ambati, J. Drusen complement component C3a and C5a promote choroidal neovascularization. *Proc. Natl. Acad. Sci. USA.* **2006**, 103, 2328–2333
23. Klein, R.J.; Zeiss, C.; Chew, E.Y.; Tsai, J.Y.; Sackler, R.S.; Haynes, C.; Henning, A.K.; sanGiovanni, J.P.; Mane, S.M.; Mayne, S.T.; Bracken, M.B.; Ferris, F.L.; Ott, J.; Barnstable, C.; Hoh, J. Complement factor H polymorphism in age-related macular degeneration. *Science.* **2005**, 308, 385–389
24. Lyzogubov, V.V.; Tytarenko, R.G.; Liu, J.; Bora, N.S.; Bora, P.S.; Polyethylene glycol (PEG)-induced model of choroidal neovascularization. *J. Biol. Chem.* **2011**, 286 (18), 16229–16237
25. Lyzogubov, V.V.; Bora, N.S.; Tytarenko, R.G.; Bora, P.S. Polyethylene glycol induced mouse model of retinal degeneration. *Exp. Eye Res.* **2014**, 27, 143–152
26. Shen, W. Y.; and Rakoczy, P. E. In vivo use of oligonucleotides to inhibit choroidal neovascularization in the eye. *Antisense Nucleic Acid Drug Dev.* **2001**, 11(4), 257–264
27. Bora, N. S.; Jha, P.; Lyzogubov, V. V.; Kaliappan, S.; Liu, J.; Tytarenko, R. G.; Fraser, D. A.; Morgan, B. P.; and Bora, P. S. Recombinant membrane-targeted form of CD59 inhibits the growth of choroidal neovascular complex in mice. *J. Biol. Chem.* **2010**, 285(44), 33826–33833
28. Chader GJ. Animal models in research on retinal degenerations: past progress and future hope. *Vision Res.* **2002**, 42(4), 393–399
29. Ramkumar, H. L.; Zhang, J.; Chan, C. C. Retinal ultrastructure of murine models of dry age-related macular degeneration (AMD). *Prog. Ret. Eye Res.* **2010**, 29(3), 169–190
30. Keeler, C.E. The inheritance of a retinal abnormality in white mice. *Proc. Natl. Acad. Sci.* **1924**, 10, 329–333
31. Hafezi, F.; Grimm, C.; Simmen, B.C.; Wenzel, A.; Remé, C.E. Molecular ophthalmology: an update on animal models for retinal degenerations and dystrophies. *Br. J. Ophthalmol.* **2000**, 84, 922–927
32. Chang, B.; Hawes, N.L.; Hurd, R.E.; Wang, J.; Howell, D.; Davisson, M.T.; Roderick, T.H.; Nusinowitz, S.; Heckenlively, J.R. Mouse models of ocular diseases. *Vis. Neurosci.* **2005**, 22, 587–593
33. Killingsworth, M. C. Angiogenesis in early choroidal neovascularization secondary to age-related macular degeneration. *Graefes Arch. Clin. Exp. Ophthalmol.* **1995**, 233(6), 313–323
34. Baba, T.; Bhutto, I. A.; Merges, C.; Grebe, R.; Emmert, D.; McLeod, D. S.; Armstrong, D.; and Lutty, G. A. A rat model for choroidal neovascularization using subretinal lipid hydroperoxide injection. *Am. J. Pathol.* **2010**, 176(6), 3085–3097
35. Zhao, L.; Wang, Z.; Liu, Y.; Song, Y.; Li, Y.; Laties, A. M.; Wen, R. Translocation of the retinal pigment epithelium and formation of sub-retinal pigment epithelium deposit induced by subretinal deposit. *Mol. Vis.* **2007**, 14(13), 873–880
36. Cao, J.; Zhao, L.; Li, Y.; Liu, Y.; Xiao, W.; Song, Y.; Luo, L.; Huang. D.; Yancopoulos, G. D.; Wiegand, S. J.; and Wen, R. A subretinal Matrigel rat choroidal neovascularization (CNV) model and inhibition of CNV and associated inflammation and fibrosis by VEGF trap. *Invest. Ophthalmol. Vis. Sci.* **2010**, 51(11), 6009–6017
37. Palarasah. Y.; Skjodt, K.; Brandt, J.; Teisner, B.; Koch, C.; Vitved, L.; and Skjoedt M. O. Generation of a C3c specific monoclonal antibody and assessment of a C3c as a putative inflammatory marker divided from complement factor C3. *J. Immunol. Methods.* **2010**, 362(1-2), 142–150
38. Haddad, S.; Chen, C. A.; Santangelo, S. L.; and Seddon, J. M. The genetics of age-related macular degeneration: a review of progress to date. *Surv. Ophthalmol.* **2006**, 51, 316–363
39. Donoso, L. A.; Kim, D.; Frost, A.; Callahan, A.; and Hageman, G. The role of inflammation in the pathogenesis of age-related macular degeneration. *Surv. Ophthalmol.* **2006**, 51, 137–152
40. Thurman, J. M.; Renner, B.; Kunchithapautham, K.; Ferreira, V. P.; Pangburn, M. K.; Ablonczy, Z.; Tomlinson, S.; Holers, V. M.; and Rohrer, B. Oxidative stress renders retinal pigment epithelial cells susceptible to complement-mediated injury. *J. Biol. Chem.* **2009**, 284, 16939–16947
41. Bai, Y. J.; Huang, L. Z.; Xu, X. L.; Du, W.; Zhou, A. Y.; Yu, W. Z.; and Li, X. X. Polyethylene glycol-modified pigment epithelial-derived factor: new prospects for treatment of retinal neovascularization. *J. Pharm. Exp. Ther.* **2012**, 342(1), 131–139
42. Fernandez-Bueno, I.; Alonso-Alonso, M. L.; Garcia-Gutierrez, M. T.; and Diebold, Y. Reliability and reproducibility of a rodent model of choroidal neovascularization based on the subretinal injection of polyethylene glycol. *Mol. Vision.* **2019**, 25, 194–203
43. Grossniklaus, H.E.; Kang, S.J.; Berglin, L. Animal models of choroidal and retinal neovascularization. *Prog. Retin. Eye Res.* **2010**, 29, 500–519

 doi:10.20944/preprints202307.1318.v1